5812 *Macromolecules* **1993**, *26*, 5812-5815

Morphology and Miscibility of Miktoarm Styrene-Diene Copolymers and Terpolymers

N. Hadjichristidis and H. Iatrou

Department of Chemistry, University of Athens, Panepistimiopolis, Athens 157 71, Greece

S. K. Behal, J. J. Chludzinski, M. M. Disko, R. T. Garner, K. S. Liang, D. J. Lohse,* and S. T. Milner

Corporate Research Laboratories, Exxon Research and Engineering Company, Annandale, New Jersey 08801

Received March 8, 1993
Revised Manuscript Received July 6, 1993

Much is known about the structure and order-disorder transitions of linear block copolymers.[1-3] Detailed information about the kinds of microphase domain morphologies that can be found in block polymers, the composition of copolymer that display each structure, and the conditions for the transitions between these morphologies, as well as into a disordered state, is available. For graft polymers, there has been only one theoretical treatment of microphase separation[4] and no experimental work, since well-defined polymers of this type have not been available. Reference 4 also discusses the order-disorder transition of starblock polymers, which are star polymers having identical diblock copolymers for arms. While the number of arms has an effect on the ordering transition, this is still predicted to be symmetrical with respect to composition. This has been confirmed experimentally.[5,6]

It has recently been shown that it is possible to synthesize nonlinear polymers that are made up of polymeric blocks with different chemical natures that are covalently linked.[7] These "miktoarm" polymers are three- or four-arm stars where the arms can be made from distinct polymeric species. This paper examines the microphase separation of such polymers and compares it to the behavior of linear block copolymers.

Polymer Synthesis. The synthesis of the 3-miktoarm star terpolymer SIB, published elsewhere by Iatrou and Hadjichristidis,[7] was performed according to the following basic reactions:

$$\mathrm{PILi} + \text{excess } \mathrm{CH_3SiCl_3} \rightarrow \underset{\mathbf{I}}{\mathrm{(PI)Si(Cl_2)CH_3}} + \mathrm{LiCl} + \mathrm{CH_3SiCl_3}\uparrow$$

$$\mathbf{I} + \mathrm{PSLi} \xrightarrow{\text{titration}} \underset{\mathbf{II}}{\mathrm{(PI)(PS)SiClCH_3}}$$

$$\mathbf{II} + \text{excess } \mathrm{PBdLi} \rightarrow \underset{\mathrm{SIB}}{\mathrm{(PI)(PS)(PBd)SiCH_3}}$$

The synthesis of the 3-arm miktoarm star copolymers S_2I and SI_2 will be given in detail in a forthcoming paper by Iatrou and Hadjichristidis. The basic reactions used are schematically

$$\mathrm{PALi} + \text{excess } \mathrm{CH_3SiCl_3} \rightarrow \underset{\mathbf{III}}{\mathrm{(PA)Si(Cl_2)CH_3}} + \mathrm{LiCl} + \mathrm{CH_3SiCl_3}\uparrow$$

$$\underset{\text{A, B: PS or PI}}{\mathbf{III} + \text{excess } \mathrm{PBLi}} \rightarrow \underset{\mathrm{S_2I \text{ or } SI_2}}{\mathrm{(PA)(PB)_2SiCH_3}} + \mathrm{LiCl}$$

The architecture of each of these miktoarom polymers is sketched in Figure 1 to give an idea of their structure. The molecular weight characterization of these polymers is given in Table I.

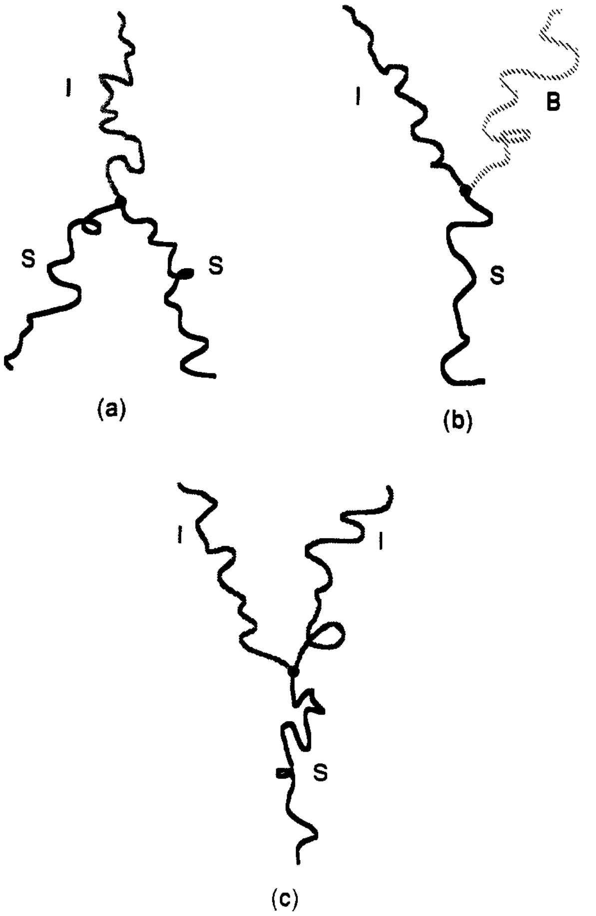

Figure 1. Structures of miktoarm polymers: (a) S_2I; (b) SIB; (c) SI_2.

Table I. Characteristics of the Miktoarm Star Co- and Terpolymers

	$M_n \times 10^3$						
sample	PS arm[a]	PI arm[a]	PBd arm[a]	miktoarm	M_w/M_n[b]	wt % PS	vol % PS
S_2I	25.9	15.9		65	1.06	76	74
SI_2	21.7	15.9		51	1.06	40	37
SIB	20.7	15.6	12.2	45.4	1.03	43	40

[a] Membrane osmometry in toluene at 35 °C. [b] SEC in THF at 30 °C.

Table II. T_g and Spacing of Miktoarm Polymers

sample	T_g^1 (°C)[a]	T_g^2 (°C)[a]	a_{cvl} (nm)[b]	A_{cvl} (nm^2)[c]
S_2I	-67.0	95.3	28.2	7.77
SI_2	-57.7	44.3	28.6	7.51
SIB	-77.9	58.4	30.7	6.42

[a] By DSC. [b] Cylindrical lattice spacing as measured by SAXS. [c] Average area per junction.

Differential Scanning Calorimetry. The glass transitions of the miktoarm polymers were measured on a Seiko 220C DSC. In all cases the sample was pressed and then annealed at room temperature for several days. It then was quenched to -100 °C, and a thermogram was taken as it was heated to 150 °C at 10 °C/min. It was again cooled rapidly to -100 °C, and a second thermogram was measured during a second heating. The T_g's of the polydiene were generally the same from both heats; the polystyrene T_g was only apparent in the first heat. These results are listed in Table II.

Small-Angle X-ray Scattering. Samples of each polymer suitable for SAXS and microscopic studies were

0024-9297/93/2226-5812$04.00/0

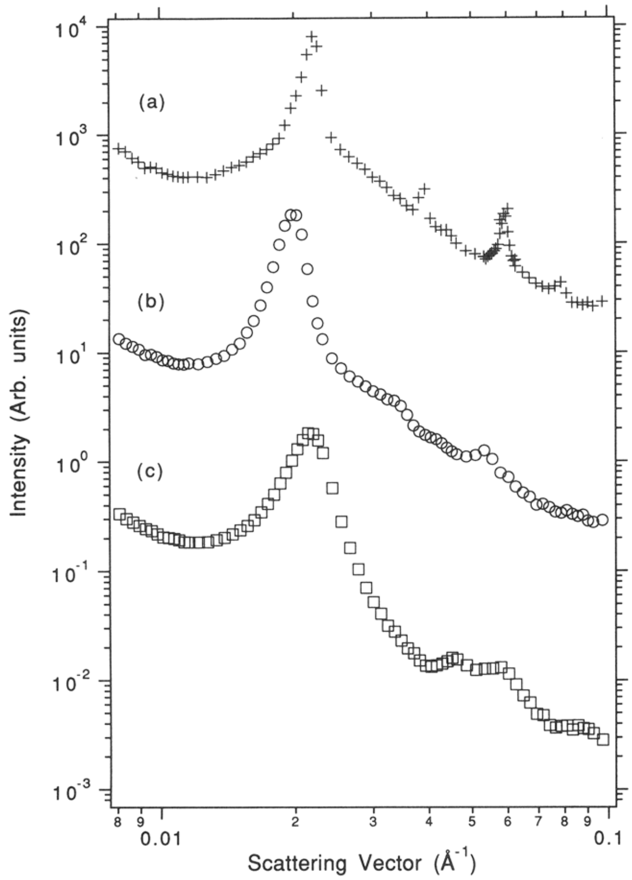

Figure 2. Small-angle X-ray scattering patterns from (a) S_2I, (b) SIB, and (c) SI_2.

made by casting films according to the procedure used by Winey.[8] Dilute (5%, w/v) solutions of each polymer in toluene were made and covered, and then the solvent was allowed to evaporate slowly over 1 week to 10 days. The toluene was fully removed by keeping the samples in a vacuum oven at 50 °C for 2 weeks, and then they were annealed in a vacuum oven at 125 °C for 1 week. The oven temperature was then slowly (over several hours) brought down to room temperature before removal of the samples. This annealing procedure was used in an effort to yield a well-ordered, equilibium morphology. SAXS measurements were carried out on these samples by using a Bonse–Hart type high-resolution setup at the Exxon Beamline X10A at the National Synchrotron Light Source at Brookhaven National Laboratory. The SAXS patterns obtained from these samples were generally consistent with a two-dimensional hexagonal arrangement of cylinders (see Figure 2). From the (100) diffraction peak, the average spacing of the samples can be found (Table II).

Transmission Electron Microscopy. All three polymers were studied by TEM. Thin sections were cryomicrotomed from the cast films described above and then stained with OsO_4 for 4 h. Since the OsO_4 reacts with unsaturation, the polydienes stain strongly while the polystyrene does not. They were then examined using a Philips EM420 TEM operated at an accelerating voltage of 100 kV. Examples of the morphologies seen are given in Figure 3. All three of those shown clearly display the hexagonal packing of a cylindrical morphology, with spacings consistent with the SAXS results.

Glass Transitions. In each sample only two T_g's were seen, even when there were three separate arms (SIB, with PS, PI, and PB arms). The high-temperature T_g corresponds well with what would be expected for PS at the molecular weights given for the arms.[9] For S_2I, one should consider a linear polymer of molecular weight equal to the sum of those for the two PS arms to understand the high-temperature T_g. There is a slight suppression of these values compared to what would be seen in homopolymer PS of the same M_w, which is expected for block polymers.

Only one low-temperature T_g was seen in each sample. For S_2I and SI_2, the value was again what one would expect for the polydiene block, again using the full molecular weight in the case of the last two polymers. It is interesting to note that SIB also showed a single low T_g, indicating that the PI and PB arms were well mixed. Using the values of the Flory interaction parameter, χ, between PI and PB measured by Sakurai et al.,[10] we estimate that χN for the PI and PB in SIB has a value less than 1 at room temperature and slightly above 1 at 120 °C where the samples were annealed. This means that they should indeed be expected to mix with each other.[4] To test whether the miktoarm chain architecture has any additional effect either promoting or impeding the miscibility of the arms, we will need to look at significantly higher molecular weights.

Morphology. All three of the samples showed cylindrical morphologies with very similar spacings of about 30 nm by TEM. This was confirmed by SAXS. The higher order diffraction peaks in the SAXS pattern for S_2I were relatively strong, indicating a high degree of long-range order; those from SI_2 and SIB were weaker, corresponding to a more disordered structure (Figure 2). The average area per junction was calculated in each case and is listed in Table II. The values of 5.40–6.57 nm^2 are indeed consistent with a cylindrical morphology.[11] The SIB sample showed only two microphases, presumably corresponding to an unstained PS phase and a second one containing the PI and PB. This is consistent with the mixing of the PI and PB arms discussed above. What is

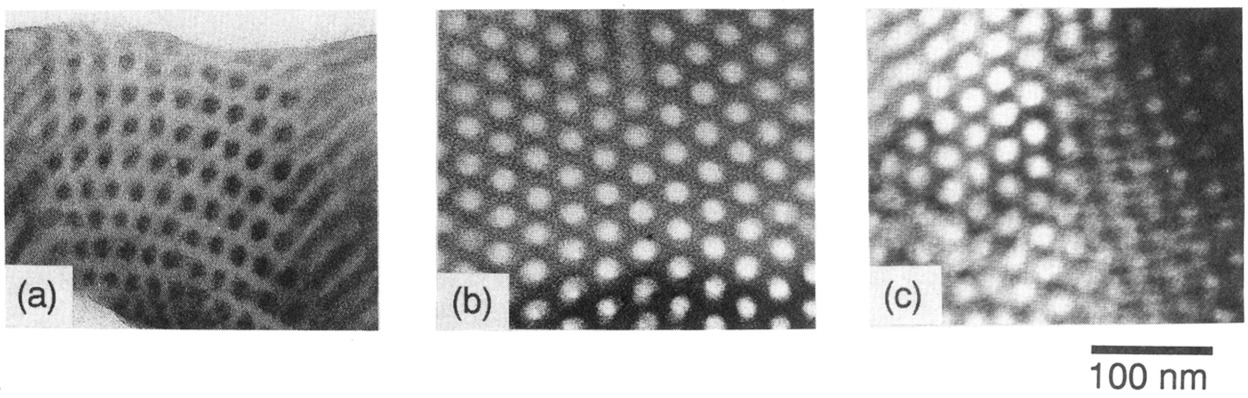

Figure 3. Transmission electron micrographs of miktoarm polymers: (a) S_2I; (b) SIB; (c) SI_2. The scale bar is 100 nm.

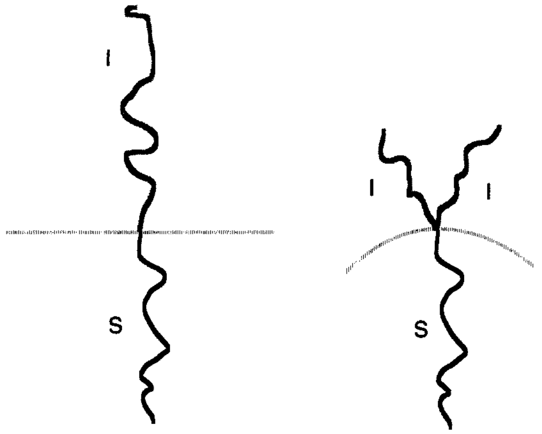

(a) (b)

Figure 4. Model for differences between the morphology of (a) the SI diblock and (b) the SI_2 miktoarm polymer. The greater crowding on the PI side of the interface for the miktoarm case leads to a greater degree of curvature.

most intriguing is that both SI_2 and SIB would be expected to have lamellar or bicontinuous structures, based on the results of linear or star-shaped block polymers.[1-3] Since the PS content is 37 and 40 vol %, respectively, for these two polymers, it is surprising that the PS was found as cylinders in these samples.

One might be able to explain how the architecture of the chains changes the ability to form domains on the basis of the model in Figure 4. Since each PS arm is attached to two polydiene arms for these miktoarm polymers, as opposed to just one for a linear diblock, there will be more crowding on the polydiene side of the interface. This will favor a higher degree of curvature, which in turn would increase the possibility of discrete PS domains in the miktoarm case. It is clear that the architecture of the chain can have a strong effect on the kinds of microphase domain structures that are found. Some understanding of the origin of this can be found in the following arguments.

Theory. Previous studies of block copolymer mesophases have typically studied AB diblock copolymers and identified a characteristic sequence of phases as the volume fraction f of A monomers is varied.[1-3] The phase diagram for strongly-segregated polymers has been calculated by Semonov[12] for diblocks; the center of the lamellar phase is by symmetry at $f = 1/2$. Clearly, the present experimental results show that changing the architecture of the chains from AB diblocks to A_2B miktoarm polymers alters the phase boundaries in the parameter f. (The following arguments apply equally well to SIB, given the miscibility of the PI and PB arms demonstrated above.) A corresponding strong-segregation phase diagram may be calculated, following Semonov.[12] As an indication of the way such a calculation might proceed, we give a simple argument for the location of the center of the lamellar phase. A single layer of strongly-segregated A_2B miktoarm polymer will have a spontaneous radius of curvature, unless the fraction f of A monomers is properly chosen. The condition for zero spontaneous curvature should be a good indication of the center of the lamellar phase.

The free energy of the layer may be written as the sum of the free energies of the two sides, each of which may be considered in strong segregation to be a melt brush. For an A_2B miktoarm polymer like the ones described above, one side has twice as many chains per area as the other side. The free energy per chain f of a curved melt brush has the form

$$f(r) \propto h^2/R^2(1 + \beta h/r + ...) \qquad (1)$$

where h is the thickness of the brush when it is flat, r is the radius of curvature, β is a numerical constant, and R is the radius of gyration of the block.

The thickness h is given in terms of the number of chains per area as

$$h = V\sigma \qquad (2)$$

where V is the volume displaced by one arm, and σ is the number of arms per area. The total free energy per chain of a curved layer of A_2B miktoarm polymer is then of the form

$$f_M(r) \propto h_B^2/R_B^2(1 + \beta h_B/r + ...) + 2h_A^2/R_A^2(1 - \beta h_A/r + ...) \qquad (3)$$

where the subscripts A and B refer to the A and B arms of the A_2B miktoarm polymer. The factor of 2 appears in the second term in eq 3 because there are two A blocks for every B block. The layer has no tendency to bend when the coefficient of $1/r$ vanishes in the expansion of $f_M(r)$ (eq 3). Noting that $\sigma_A = 2\sigma_B$, this coefficient vanishes when

$$V_B^3/R_B^2 = 16V_A^3/R_A^2 \qquad (4)$$

This represents a bilayer with zero spontaneous curvature, which we expect to correspond to the middle of the lamellar region.

This may be written in a useful form as follows. The length between entanglements in a one-component polymer melt, l, has been observed to scale as V/R^2, with prefactors independent of the choice of polymer. (This scaling law has been argued theoretically by several authors;[13-16] it follows, for instance, from the assertion that an entanglement results from a strand of polymer long enough that the volume swept out by that strand is just large enough to contain another such strand.) Using this relation and eqs 2 and 4, we may write a geometrical condition for the absence of spontaneous curvature as

$$h_B = 2h_A(l_A/l_B)^{1/2} \qquad (5)$$

If the polymers are elastically indentical, $l_A = l_B$ and we see that for such idealized A_2B miktoarm polymers, the B layer must be twice as thick as the A layer to achieve zero spontaneous curvature. The A layer thus has a strong preference to be on the outside of a curved surface. This means that for such A_2B miktoarm polymers the center of the lamellar region is where the volume fraction of A is about 33%, rather than 50% in the AB diblock case.

It is useful at this point to compare the case of these miktoarm polymers with that of the starblocks. As mentioned above, the phase behavior of the starblocks also differs from that of linear block polymers.[4-6] However, the starblocks do not show the strong asymmetry with respect to composition that the miktoarms do. This is because the starblocks do not have the basic asymmetry on numbers of each kind of arm, having an equal number of each kind. In the strong segregation limit, the central junction of the starblock is restricted to the center of one of the kinds of lamellae (i.e., that made up of the central blocks).[17] In the same limit, however, the ends of diblock chains are also found in the center of the lamellae, so there is very little difference in the stretching energies between starblock and linear block polymers. In contrast, as we have shown herein, there are significant differences between each of those cases and that of the miktoarm star polymers.

This result gives an indication of how copolymer architecture may be used to alter the relation between the microstructure and volume fraction of the two blocks. It may be desirable, for instance, to obtain a microstructure in which a minority component is nonetheless continuous (or equivalently in which a majority component is discontinuous). This may be achieved by A_2B miktoarm polymers (or other related structures), because the long single block will favor the inwardly curved side of interfaces even if it is the majority component.

Summary. The microphase separation of the new miktoarm styrene–diene polymers has been examined. At the molecular weights studied, the PS arms always separate from the polydienes, but the PI and PB arms mix when they occur in the same molecule. This is the kind of behavior that would be expected from experience with linear diblocks. On the other hand, the miktoarm architecture does seem to strongly affect the kind of microphase-separated domains that are formed in these polymers. The polymers with a single PS arm and two polydiene arms formed PS cylinders, whereas a lamellar or bicontinuous structure would have been expected from literature on linear block polymers. This appears to be due to effects of the miktoarm structure on the curvature energy of the interface.

References and Notes

(1) Molau, G. E. *Block Copolymers*; Agarwal, S. L., Eds.; Plenum: New York, 1970.

(2) Thomas, E. L.; Anderson, D. M.; Henkee, C. S.; Hoffman, D. *Nature* **1988**, *334*, 598.

(3) Bates, F. S.; Fredrickson, G. H. *Annu. Rev. Phys. Chem.* **1990**, *41*, 525.

(4) Olvera de la Cruz, M.; Sanchez, I. C. *Macromolecules* **1986**, *19*, 2501.

(5) Alward, D. B.; Kinning, D. J.; Thomas, E. L.; Fetters, L. J. *Macromolecules* **1986**, *19*, 215.

(6) Hashimoto, T.; Ijichi, Y.; Fetters, L. J. *J. Chem. Phys.* **1989**, *89*, 2463.

(7) Iatrou, H.; Hadjichristidis, N. *Macromolecules* **1992**, *25*, 4649.

(8) Winey, K. I. Ph.D. Thesis, University of Massachusetts, Amherst, MA, 1991.

(9) Fox, T. G.; Flory, P. J. *J. Polym. Sci.* **1954**, *14*, 315.

(10) Sakurai, S.; Jinnai, H.; Hasegawa, H.; Hashimoto, T.; Han, C. C. *Macromolecules* **1991**, *24*, 4839.

(11) Winey, K. I.; Thomas, E. L.; Fetters, L. J. *J. Chem. Phys.* **1991**, *95*, 9367.

(12) Semonov, A. N. *Sov. Phys. JETP* **1985**, *61*, 733.

(13) Kavassalis, T. A.; Noolandi, J. *Phys. Rev. Lett.* **1987**, *59*, 2674.

(14) Lin, Y.-H. *Macromolecules* **1987**, *20*, 3080.

(15) Fetters, L. J.; Lohse, D. J., to be published.

(16) Witten, T. A., private communication.

(17) Milner, S. T.; Witten, T. A. *Macromolecules* **1992**, *25*, 5495.